

Casimir force between eccentric cylinders

D. A. R. DALVIT¹, F. C. LOMBARDO², F. D. MAZZITELLI² and R. ONOFRIO^{3,4}

¹ *Theoretical Division, MS B213, Los Alamos National Laboratory
Los Alamos, NM 87545, USA*

² *Departamento de Física J. J. Giambiagi, Facultad de Ciencias Exactas y Naturales
Universidad de Buenos Aires - Ciudad Universitaria, Pabellón I
1428 Buenos Aires, Argentina*

³ *Department of Physics and Astronomy, Dartmouth College
6127 Wilder Laboratory, Hanover, NH 03755, USA*

⁴ *Dipartimento di Fisica “G. Galilei”, Università di Padova
Via Marzolo 8, Padova 35131, Italy*

(received 25 March 2004; accepted in final form 9 June 2004)

PACS. 03.70.+k – Theory of quantized fields.

PACS. 42.50.Pq – Cavity quantum electrodynamics; micromasers.

PACS. 04.80.Cc – Experimental tests of gravitational theories.

Abstract. – We consider the Casimir interaction between a cylinder and a hollow cylinder, both conducting, with parallel axis and slightly different radii. The Casimir force, which vanishes in the coaxial situation, is evaluated for both small and large eccentricities using the proximity approximation. The cylindrical configuration offers various experimental advantages with respect to the parallel planes or the plane-sphere geometries, leading to favourable conditions for the search of extra-gravitational forces in the micrometer range and for the observation of finite-temperature corrections.

Casimir forces are one of the most striking macroscopic manifestations of vacuum quantum fluctuations. Recently, there has been an increasing interest in experimental and theoretical aspects of these forces [1]. The force between parallel conducting plates as originally predicted in [2], after a first evidence reported in [3], has recently been measured at the 15% accuracy level using cantilevers [4]. A force of similar nature between a conducting plane and a conducting sphere, after pioneering studies [5], has also been investigated with progressively higher precision and accuracy. The latter force has been measured by using torsion balances [6], atomic force microscopes [7], and micromechanical resonators whose motion was detected through capacitance bridges [8] and fiber optic interferometers [9]. Casimir forces may be relevant in nanotechnology, giving rise to interesting non-linear dynamics for nanoelectromechanical systems [10]. Also, the predicted existence of new interactions with coupling comparable to gravity but range in the micrometer region [11] adds strong motivations to control the Casimir force at the highest level of accuracy. This requires taking into account many deviations from the ideal situation initially discussed in [2], among these the corrections due to roughness and finite conductivity of the metallic surfaces, and the effect of the finite temperature, somewhat

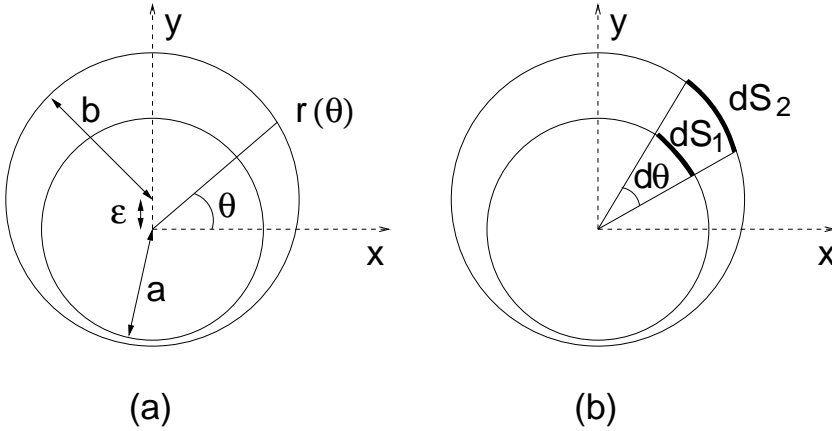


Fig. 1 – Cylindrical geometry for measuring Casimir forces. (a) An inner cylinder of radius a and a hollow cylinder of radius b , with the origin of coordinates on the axis of the inner cylinder, and distance ϵ between the two axes. The function $r(\theta)$ gives the radial coordinate of the outer cylinder from the axis of the inner one. (b) The effective area for the application of the proximity approximation, as the geometric mean of dS_1 and dS_2 : $dA_{\text{eff}}(\theta) = \sqrt{dS_1 dS_2}$.

controversial [12,13], yet to be observed. Moreover, the observation of the thermal contribution is important in itself as a macroscopic test of quantum field theories at finite temperature.

In this paper we analyze a geometry different from the previously studied cases of two parallel planes or a plane-sphere. We consider one conducting cylinder inserted inside a hollow conducting cylinder, with parallel axis. In the ideal coaxial case, the two axes will coincide and, based on symmetry arguments, this will result in a null Casimir force, while in the general eccentric case a finite force will arise. This configuration may be useful to minimize spurious gravitational and electromagnetic effects, and has specific advantages with respect to the parallel plane and the plane-sphere geometries. The discussion will naturally lead to some proposal for experimental schemes which should allow to get more stringent limits to extra-gravitational forces in the micrometer range or to achieve an easier observation of the finite-temperature corrections to the Casimir force.

Let us consider two eccentric cylinders of length L , with radii a and b , respectively (with $L \gg a, b$ to neglect border effects), as depicted in fig. 1. We will mainly focus on the particular case $a \simeq b$, since in this case the Casimir force is enhanced. The distance between the axes of the cylinders, a measure of the eccentricity, will be denoted by ϵ . In order to evaluate the Casimir energy we will use the proximity approximation [14]. This is partially justified by recent results [15] showing that, for concentric cylinders, the proximity approximation reproduces the exact results far beyond its expected range of validity. This result holds as long as one uses the geometric mean prescription for the effective area [16], a prescription which arises naturally in a semiclassical framework [15,17]. It is then reasonable to assume that this is also true at least for slightly eccentric cylinders (the proximity force approximation could be improved using the geometric optics approach put forward in [18], or the numerical method of [16]).

From the Casimir energy per unit area for parallel plates separated by a distance l ,

$$E_{\text{pp}}^{(0)}(l) = -\frac{\pi^2 \hbar c}{720 l^3}, \quad (1)$$

the interaction energy between cylinders is, using the proximity approximation,

$$E_1^{(0)} \simeq \int_0^{2\pi} dA_{\text{eff}}(\theta) E_{\text{pp}}^{(0)}(r(\theta) - a), \tag{2}$$

where $r(\theta)$ is the distance of a point of the external cylinder to the axis of the inner one, and $dA_{\text{eff}}(\theta)$ is the geometric mean of two infinitesimal adjacent areas on both cylinders. Following the notations introduced in fig. 1, we find that $r(\theta) = \sqrt{b^2 - \epsilon^2 \cos^2 \theta} + \epsilon \sin \theta$ and $dA_{\text{eff}} = L\sqrt{ab} + \epsilon a \sin \theta d\theta$. The interaction energy and the force between the two cylinders $F_y^{(0)} = -\partial E_1 / \partial \epsilon$ depend on the dimensionless parameters ϵ/b and $\tilde{\epsilon} = \epsilon/(b - a)$. Since we are considering $a \simeq b$, we will always have $\epsilon/b \ll 1$ and $\tilde{\epsilon} \gg \epsilon/b$. Thus to lowest order in ϵ/b we obtain

$$F_y^{(0)} = -\frac{\pi^2 \hbar c L a}{240(b - a)^4} \int_0^{2\pi} \frac{d\theta \sin \theta}{(1 + \tilde{\epsilon} \sin \theta)^4} \simeq \tilde{\epsilon} \frac{1 + \frac{\tilde{\epsilon}^2}{4}}{(1 - \tilde{\epsilon}^2)^{\frac{7}{2}}} F_0, \tag{3}$$

where $F_0 = -\pi^3 \hbar c L a / 60(b - a)^4$ is twice the equivalent Casimir force between two parallel plates with the same area of the two cylinders and spaced by a distance $b - a$. It is worth noting that the force always makes the equilibrium position of ideal coaxial cylinders unstable.

For nearly concentric cylinders, $\tilde{\epsilon} \ll 1$, the force is linear in the distance between the axes of the cylinders:

$$F_y^{(0)} \simeq \frac{\epsilon}{b - a} F_0. \tag{4}$$

This corresponds to an inverted harmonic oscillator, and explicitly shows the instability. In the opposite case, when $\tilde{\epsilon} \rightarrow 1$, we get

$$F_y^{(0)} \simeq \frac{5}{32\sqrt{2}} \left(\frac{b - a}{d} \right)^{7/2} F_0, \tag{5}$$

where $d = b - a - \epsilon$ is the distance between the cylinders. The behavior of the force in the large eccentricity limit $\tilde{\epsilon} \rightarrow 1$ is similar to that of a cylinder parallel to a plane. Indeed, with a cylinder of radius a at a distance $d \ll a$ from a plane, the force is

$$F_{\text{cp}}^{(0)}(d) \simeq -\frac{\pi^2 \hbar c L}{120a^3} \int_0^{\pi/2} \frac{d\theta}{(1 + \frac{d}{a} - \cos \theta)^4} \simeq -\frac{\pi^3 \hbar c L a^{1/2}}{384\sqrt{2}d^{7/2}}. \tag{6}$$

The scaling of the Casimir force with distance is intermediate between the *plane-spherical* ($\propto d^{-3}$) and the parallel plate configuration ($\propto d^{-4}$), as well as the absolute force signal, for typical values of the geometrical parameters. Indeed, the relative strengths of the forces for a common distance d between the two bodies are

$$\begin{aligned} \frac{F_{\text{pp}}^{(0)}(d)}{F_{\text{cp}}^{(0)}(d)} &= \frac{0.72A}{L(ad)^{1/2}}, \\ \frac{F_{\text{cp}}^{(0)}(d)}{F_{\text{sp}}^{(0)}(d)} &= \frac{0.66L}{R} \left(\frac{a}{d} \right)^{1/2}, \end{aligned} \tag{7}$$

where $F_{\text{pp}}^{(0)}$ is the force between parallel plates of area A , $F_{\text{sp}}^{(0)}$ is the force between the sphere and the plane, with R the radius of the sphere. If, for instance, we choose $A = 1 \text{ mm}^2$, $a = R = 100 \mu\text{m}$, $L = 5 \text{ mm}$ and $d = 1 \mu\text{m}$, the Casimir force ratios are $F_{\text{pp}}^{(0)} / F_{\text{cp}}^{(0)} \simeq 14$ and

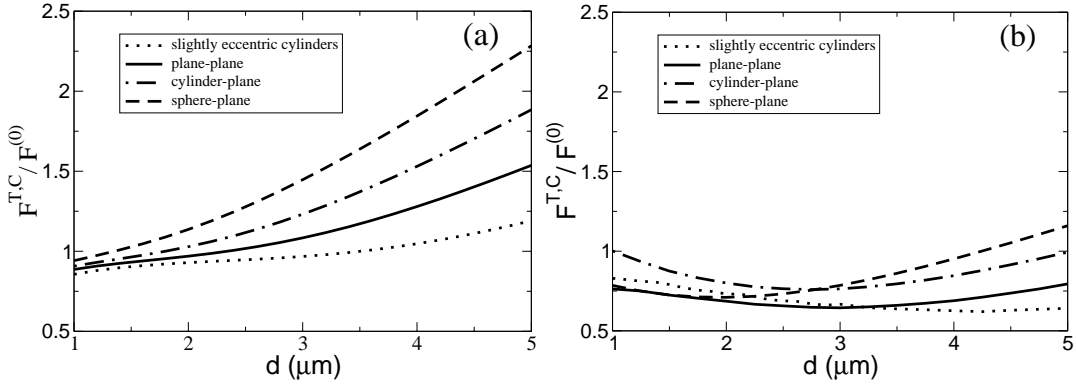


Fig. 2 – Combined thermal and conductivity corrections to the Casimir force for various geometries. We depict the relative contributions $F^{T,C}/F^{(0)}$ vs. the distance d between gold metallic surfaces in the case of slightly eccentric cylinders, cylinder-plane, plane-plane, and sphere-plane configurations, for two different finite-conductivity scenarios, the so-called plasma model (a) [19] and a model that excludes the zero-frequency TE mode (b) [13]. For both figures parameters are $a = R = 100 \mu\text{m}$ and $T = 300 \text{K}$.

$F_{\text{cp}}^{(0)}/F_{\text{sp}}^{(0)} \simeq 330$. With respect to the plane-spherical situation, one can enhance the signal by exploiting the linear dimension, *i.e.* the size L , at least as far as the parallelism between the axes of cylinder and plane or their surface roughness do not become an issue.

For an accurate comparison between experiment and theory we need to consider the deviations of the predicted force from the ideal situation of perfect conductors, zero temperature, and zero roughness. For typical surfaces and realistic experimental sensitivities, roughness corrections are not relevant at the distances we are interested in ($d > 1 \mu\text{m}$). On the other hand, combined temperature and conductivity corrections are important in this range of distances. These corrections have been computed using different approaches, leading to controversial predictions for the Casimir force between parallel plates [12, 13, 19].

We have computed the combined corrections due to finite temperature and finite conductivity using two distinct theoretical models. In fig. 2a we show the combined corrections obtained using the plasma model. Our starting point is the expression for the interaction energy per unit area in the plane-plane geometry at finite temperature and finite conductivity, E_{pp} , which was derived in [19] using the plasma model for the dielectric function in the Lifshitz formula. Figure 2b depicts the combined corrections using the model described in [13], in which the transverse electric zero mode does not contribute at all to the Casimir force. Our calculation is based on fig. 4 of [13], which shows the surface force density between parallel gold metallic plates. Such force density was computed using the experimental data for the permittivity of gold as a function of frequency [20]. The results for the different geometries shown in both figures have been numerically obtained from the plane-plane configuration using the proximity force approximation. In the particular case of slightly eccentric cylinders, the Casimir force can be easily obtained from E_{pp} . Indeed, the interaction energy between cylinders is given by eq. (2), where $E_{\text{pp}}^{(0)}$ should be replaced by E_{pp} . Expanding the right-hand side of eq. (2) in powers of $\tilde{\epsilon}$, one can derive the force between nearly concentric cylinders ($\tilde{\epsilon} \ll 1$) in terms of the second derivative of the energy E_{pp} evaluated at a separation $l = b - a$, namely

$$F_y \simeq -\epsilon\pi L a \left. \frac{d^2 E_{\text{pp}}}{dl^2} \right|_{(b-a)}. \quad (8)$$

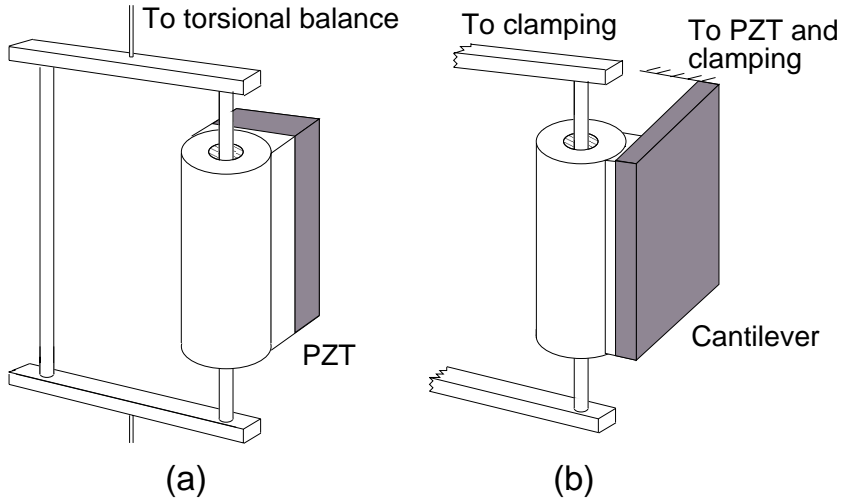


Fig. 3 – Experimental schemes for detecting Casimir forces with slightly eccentric cylinders. (a) The inner cylinder is rigidly connected to a torsional balance and the signal to restore the zero eccentricity configuration after a controlled displacement is monitored. (b) The hollow cylinder is connected to a cantilever and the frequency shift induced in the small oscillations is measured.

We see that, in the range where temperature corrections can be more likely observable (above $\simeq 3 \mu\text{m}$), both models predict the same hierarchy for the various geometries, with the larger relative correction for the sphere-plane, followed by the cylinder-plane, plane-plane, and slightly eccentric cylinders, respectively. At the same time, the corrections in the same range of distances are significantly different to allow for a crucial test of the models, with an enhancement and a depletion of the measurable force with respect to the zero-temperature case for the two models, respectively, resulting in predicted forces differing by almost a factor 2. The absolute magnitude of the force in the plane-cylindrical case is much larger than that of the sphere-plane situation and, with respect to the parallel plates, there are less issues of dust and parallelism, making this configuration more favourable for looking at thermal corrections. Instead, in the case of slightly eccentric cylinders the corrections are weaker than those in the other three geometries, making this configuration more robust for seeking extra-gravitational forces with suppressed background

We now discuss possible experimental arrangements for measuring the Casimir force between cylinders. In the case of the almost coaxial configuration $\tilde{\epsilon} \ll 1$, one possibility is to repeat a microscopic version of the experiment described in [21] to test universal gravitation in the cm range, with a small torsional balance mounted on the ends of the internal cylinder. In this case, the unstable force could be evidenced by intentionally creating a controlled eccentricity and measuring the feedback force required to bring the internal cylinder to zero eccentricity, as depicted in fig. 3a. A somewhat simpler situation can be imagined by attaching the external hollow cylinder to a cantilever, then creating a resonator of effective mass M and natural angular frequency ω_0 , see fig. 3b. In the presence of the inner cylinder (kept in a fixed position), the frequency of the resonator for small oscillations around the equilibrium position is renormalized by the negative spring constant of the Casimir force (see eq. (4)). Assuming a small frequency shift (*i.e.* a Casimir force much smaller than the restoring force of the resonator), and achievable values $a = 100 \mu\text{m}$, $L = 5 \text{ mm}$, $M = 10^{-6} \text{ kg}$, $b - a = 1 \mu\text{m}$ and $\omega_0 = 10^3 \text{ s}^{-1}$, we obtain $\Delta\omega/\omega_0 = -F_0/2(b-a)M\omega_0^2 = -4.25 \times 10^{-3}$, which is within the sensitivity of frequency-shift techniques on microresonators [9, 22].

This configuration has some advantages over the parallel-plates geometry. If there is no residual charge in the inner cylinder, the system remains neutral and screened by the external one from background noise sources, and from residual charges in the outer cylinder. When the inner cylinder has a residual charge, there will be a small potential difference V between the cylinders, and the coaxial configuration will be electrostatically unstable. The Laplace equation for the electrostatic potential ϕ in the region between the two cylinders can be solved by imposing the boundary conditions $\phi(a, \theta) = 0$ and $\phi(r(\theta), \theta) = V$. To first order in ϵ/b we find

$$\phi(r, \theta) \simeq \frac{V}{\log(b/a)} \left[\log\left(\frac{r}{a}\right) - \epsilon \frac{r^2 - a^2}{b^2 - a^2} \frac{\sin \theta}{r} \right]. \quad (9)$$

The electrostatic force between cylinders can be computed as $F_y^E \simeq \epsilon_0 \pi V^2 L a \epsilon / (b-a)^3$, where ϵ_0 is the electric permittivity of vacuum. This result, which shows the electrostatic instability, can also be obtained from $F_y^E = -(\partial U_E / \partial \epsilon)_V$, using a proximity approximation for the electrostatic energy U_E :

$$U_E \simeq \frac{1}{2} \epsilon_0 V^2 L a \int_0^{2\pi} \frac{d\theta}{r(\theta) - a}. \quad (10)$$

The electrostatic instability can be avoided by putting the cylinders in contact, something unavoidable during the preliminary stages of parallelization. Then the residual charge of the inner cylinder will flow to the hollow cylinder, apart from a residual charge due to imperfections and finite length of the cylinders. This residual charge will be smaller than for other geometries, as the same discharging procedure does not work in the other configurations. If some residual potential difference still remains, it will contribute to the frequency shift, however it can be eliminated by a counterbias as in all the Casimir experiments performed so far. The electrostatic instability can be exploited to improve the parallelism between cylinders. One could apply a time-dependent potential between the cylinders and measure the force, as in the experiments to test the inverse-square Coulomb law. Parallelism and concentricity would be maximum for a minimum value of the force. Moreover, the expected gravitational force is obviously null, this being an advantage to look for intrinsically short-range extra-gravitational forces. These should violate the Gauss law, as could be evidenced by performing an experiment analogous to that done with macroscopic cylinders in [21].

In conclusion, we have computed the Casimir force between conducting eccentric cylinders, using the proximity approximation, also including finite-temperature and conductivity effects. Our results suggest that cylindrical configurations could be useful to precisely measure the Casimir force and related signals superimposed to it. We have briefly described experimental configurations which look promising, either to minimize spurious effects of gravitational, electrostatic, conductivity and thermal origin to search for new forces, as in the case of slightly eccentric cylinders, or for intentionally looking at finite-temperature corrections to the Casimir force, as in the cylindrical-plane configuration. Recent progress in machining nanomechanical structures should make our proposal feasible.

* * *

We would like to thank A. RONCAGLIA and P. VILLAR for computational help. This work was supported by DOE, University of Buenos Aires, CONICET, Fundación Antorchas and ANPCyT.

REFERENCES

- [1] PLUNIEN G., MÜLLER B. and GREINER W., *Phys. Rep.*, **134** (1986) 87; MILONNI P., *The Quantum Vacuum* (Academic Press, San Diego) 1994; MOSTEPANENKO V. M. and TRUNOV N. N., *The Casimir Effect and Its Applications* (Clarendon, London) 1997; BORDAG M., *The Casimir Effect 50 Years Later* (World Scientific, Singapore) 1999; BORDAG M., MOHIDEEN U. and MOSTEPANENKO V. M., *Phys. Rep.*, **353** (2001) 1; REYNAUD S. *et al.*, *C. R. Acad. Sci. Paris*, **IV-2** (2001) 1287; MILTON K. A., *The Casimir Effect: Physical Manifestations of the Zero-Point Energy* (World Scientific, Singapore) 2001.
- [2] CASIMIR H. B. G., *Proc. K. Ned. Akad. Wet. B*, **51** (1948) 793.
- [3] SPARNAAY M. J., *Physica*, **24** (1958) 751.
- [4] BRESSI G., CARUGNO G., ONOFRIO R. and RUOSO G., *Phys. Rev. Lett.*, **88** (2002) 041804.
- [5] VAN BLOKLAND P. H. G. M. and OVERBEEK J. T. G., *J. Chem. Soc. Faraday Trans. I*, **74** (1978) 2637.
- [6] LAMOREAUX S. K., *Phys. Rev. Lett.*, **78** (1997) 5.
- [7] MOHIDEEN U. and ROY A., *Phys. Rev. Lett.*, **81** (1998) 4549; HARRIS B. W., CHEN F. and MOHIDEEN U., *Phys. Rev. A*, **62** (2000) 052109.
- [8] CHAN H. B., AKSYUK V. A., KLEIMAN R. N., BISHOP D. J. and CAPASSO F., *Science*, **291** (2001) 1941.
- [9] DECCA R. S., LOPEZ D., FISCHBACH E. and KRAUSE D. E., *Phys. Rev. Lett.*, **91** (2003) 050402.
- [10] CHAN H. B., AKSYUK V. A., KLEIMAN R. N., BISHOP D. J. and CAPASSO F., *Phys. Rev. Lett.*, **87** (2001) 211801.
- [11] FISCHBACH E. and TALMADGE C. L., *The Search for Non-Newtonian Gravity* (AIP/Springer-Verlag, New York) 1999.
- [12] BOSTROM M. and SERNELIUS B. E., *Phys. Rev. Lett.*, **84** (2000) 4757; LAMOREAUX S. K., *Phys. Rev. Lett.*, **87** (2001) 139101; SERNELIUS B. E., *Phys. Rev. Lett.*, **87** (2001) 139102; CHEN F., KLIMCHITSKAYA G. L., MOHIDEEN U. and MOSTEPANENKO V. M., *Phys. Rev. Lett.*, **90** (2003) 160404; GEYER B., KLIMCHITSKAYA G. L. and MOSTEPANENKO V. M., *Phys. Rev. A*, **67** (2003) 062102; **65** (2002) 062109; ESQUIVEL R., VILLARREAL C. and MOCHAN W. L., quant-ph/0306139; MOCHAN W. L., VILLARREAL C. and ESQUIVEL-SIRVENT R., quant-ph/0206119; GENET C., LAMBRECHT A. and REYNAUD S., *Int. J. Mod. Phys. A*, **17** (2002) 761; *Phys. Rev. A*, **62** (2000) 012110; SVETOVY V. B. and LOKHANIN M. V., *Phys. Rev. A*, **67** (2003) 022113.
- [13] HØYE J. S., BREVIK I., ASRSETH J. B. and MILTON K. A., *Phys. Rev. E*, **67** (2003) 056116.
- [14] DERJAGUIN B. V. and ABRIKOSOVA I. I., *Sov. Phys. JETP*, **3** (1957) 819; DERJAGUIN B. V., *Sci. Am.*, **203** (1960) 47.
- [15] MAZZITELLI F. D., SANCHEZ M. J., SCOCCOLA N. N. and VON STECHER J., *Phys. Rev. A*, **67** (2003) 013807.
- [16] Similar results based on numerical simulations have been reported for the force between a plate and a sphere, see: GIES H., LANGFELD K. and MOYAERTS L., *J. High Energy Phys.*, **6** (2003) 018.
- [17] SCHADEN M. and SPRUCH L., *Phys. Rev. Lett.*, **84** (2000) 459; *Phys. Rev. A*, **58** (1998) 935.
- [18] JAFFE R. L. and SCARDICCHIO A., *Phys. Rev. Lett.*, **92** (2004) 070402.
- [19] KLIMCHITSKAYA G. L. and MOSTEPANENKO V. M., *Phys. Rev. A*, **63** (2001) 062108.
- [20] LAMBRECHT A. and REYNAUD S., *Eur. Phys. J. D*, **8** (2000) 309; *Phys. Rev. Lett.*, **84** (2000) 5672.
- [21] HOSKINS J. K., NEWMAN R. D., SPERO R. and SCHULTZ J., *Phys. Rev. D*, **32** (1985) 3084.
- [22] BRESSI G., CARUGNO G., GALVANI A., ONOFRIO R., RUOSO G. and VERONESE F., *Class. Quantum Grav.*, **18** (2001) 3943.